Mitochondria are an early target of oxidative modifications in senescing legume nodules

Manuel A. Matamoros[1*], Nieves Fernández-García[2], Stefanie Wienkoop[3], Jorge Loscos[1], Ana Saiz[1] and Manuel Becana[1]

[1]Departamento de Nutrición Vegetal, Estación Experimental de Aula Dei, Consejo Superior de Investigaciones Científicas (CSIC), Apartado 13034, 50080 Zaragoza, Spain; [2]Departamento de Biología del Estrés y Patología Vegetal, Centro de Edafología y Biología Aplicada del Segura, CSIC, Campus de Espinardo, Apartado 164, 30100 Espinardo-Murcia, Spain; [3]Department of Molecular Systems Biology, University of Vienna, 1090 Vienna, Austria

Received: *4 October 2012*
Accepted: *12 October 2012*

Author for correspondence: Estación Experimental de Aula Dei, Consejo Superior de Investigaciones Científicas, Apartado 13034, 50080 Zaragoza, Spain
Tel: +34-976-716064
Fax: +34-976-716145
Email: manumat@eead.csic.es

Summary: 200
Introduction: 688
Materials and Methods: 1891
Results: 2028
Discussion: 1294
Acknowledgements: 68
Main body: 5969
Number of Tables: 3
Number of Figures: 6

Summary

- Legume nodule senescence is a poorly understood process involving a decrease in N_2 fixation and an increase in proteolytic activity. Some physiological changes during nodule aging have been reported, but scarce information is available at the subcellular level.
- Biochemical, immunological, and proteomic approaches were used to provide insight into the effects of aging on the mitochondria and cytosol of nodule host cells.
- In the mitochondria, the oxidative modification of lipids and proteins was associated with a marked decline in glutathione, a reduced capacity to regenerate ascorbate, and upregulation of alternative oxidase and manganese-superoxide dismutase. In the cytosol, there were consistent reductions in the protein levels of carbon metabolism enzymes, inhibition of protein synthesis and increase in serine proteinase activity, disorganization of cytoskeleton, and a sharp reduction of cytosolic proteins, but no detectable accumulation of oxidized molecules.
- We conclude that nodule mitochondria are an early target of oxidative modifications and a likely source of redox signals. Alternative oxidase and manganese-superoxide dismutase may play important roles in controlling ROS concentrations and the redox state of mitochondria. The finding that specific methionine residues of a cytosolic glutamine synthetase isoform are sulfoxidized suggests a regulatory role of this enzyme in senescing nodules.

Key words: Antioxidants, mitochondria, nodule senescence, oxidative damage, *Phaseolus vulgaris*.

New Phytologist (2012)

Introduction

The symbiotic interaction between rhizobia and legume roots leads to the formation of N_2-fixing nodules, allowing legumes to grow under nitrogen-limiting conditions (Oldroyd & Downie, 2008). Nodules produce high amounts of reactive oxygen species (ROS) such as superoxide radicals (O_2^-) and hydrogen peroxide (H_2O_2) due to the elevated rates of respiration in bacteroids and mitochondria. These organelles are endowed with an important set of antioxidants that finely regulate ROS concentration (Iturbe-Ormaetxe *et al.,* 2001). Antioxidants prevent the oxidation of mitochondrial components and permit the participation of ROS in intracellular redox signaling (Maxwell *et al.,* 2002; Rhoads *et al.,* 2006; Noctor *et al.,* 2007).

In a previous work, the antioxidant systems of bean (*Phaseolus vulgaris*) nodule mitochondria were examined in detail (Iturbe-Ormaetxe *et al.,* 2001). It was proposed that O_2^- generated by the electron transport chain is dismutated to H_2O_2 and O_2 by a manganese superoxide dismutase (MnSOD) present in the matrix (Iturbe-Ormaetxe *et al.,* 2001; Rubio *et al.,* 2004). H_2O_2 is scavenged by either a membrane bound or by a soluble ascorbate peroxidase (APX) using ascorbate supplied by L-galactono-1,4-lactone dehydrogenase (GalLDH), which is localized in the inner membrane (Matamoros *et al.,* 2006). Oxidized ascorbate can be reduced in the matrix by NADH-dependent monodehydroascorbate reductase (MR) or by glutathione-dependent dehydroascorbate reductase (DR). In bean and some other legumes, homoglutathione may replace glutathione as electron donor in the ascorbate-glutathione pathway and probably in other thiol-related functions. Finally, reduced homoglutathione can be regenerated in the matrix by (homo)glutathione reductase (GR) using NADPH as an electron donor.

Other antioxidant enzymes have been proposed as important players in the redox signaling network of plant cells. Peroxiredoxins (Prxs) catalyze the reduction of H_2O_2 and

alkylhydroperoxides, and in so doing they probably modulate signaling cascades mediated by ROS and reactive nitrogen species such as nitric oxide (NO). In plants, there are four classes of Prxs that differ in their catalytic mechanisms and subcellular location (Dietz *et al.,* 2006). To carry out their functions as antioxidants and redox sensors, the balance between oxidized and reduced Prxs is tightly regulated. Thioredoxins (Trxs) constitute a family of proteins that perform multiple functions related to cellular redox homeostasis and may act as reductants of some Prx isoforms (Dietz *et al.,* 2006). In turn, Trxs can be reduced by NADPH-dependent Trx reductases (NTRs) in the cytosol and mitochondria (Laloi *et al.,* 2001). Recently, we have reported the presence of a NTR-Trx-Prx system in the nodules of the model legume *Lotus japonicus* (Tovar-Méndez *et al.,* 2011). In this species cytosolic PrxIIB can be regenerated by Trx*h1*, Trx*h4* and NTRs, whereas in mitochondria oxidized PrxIIF is reduced by Trx*o* and NTRs.

Senescence is a highly complex and regulated developmental process involving the degradation of organelles and macromolecules (Lim *et al.,* 2007). In legume nodules, stress-induced senescence shares several characteristics with natural or developmental senescence (aging), including the decline of N_2 fixation, leghemoglobin (Lb), and some antioxidant enzymes and metabolites, as well as the oxidative damage of cell components (Evans *et al.,* 1999; Matamoros *et al.,* 1999a; Hernández-Jiménez *et al.,* 2002; Loscos *et al.,* 2008). By contrast, recent studies with *Medicago truncatula* nodules suggest partially divergent molecular mechanisms for developmental and stress-induced senescence (Pérez-Guerra *et al.,* 2010).

Ultrastructural studies have provided insight into the events occurring at the subcellular level during nodule senescence (Matamoros *et al.,* 1999a; Hernández-Jiménez *et al.,* 2002; Rubio *et al.,* 2004; Puppo *et al.,* 2005). However, the role of cell organelles in nodule senescence is unclear. In animals, oxidative stress in mitochondria is considered a major hallmark of cellular aging. Consistent with this, transgenic mice that overexpress human catalase in mitochondria show an increased life span and delayed

age-related pathologies (Schriner *et al.,* 2005). In plants, Palma *et al.* (2006) reported an increased activity of the ascorbate–glutathione cycle enzymes and a decreased content of ascorbate in mitochondria from senescent pea (*Pisum sativum*) leaves. Nevertheless, the sequence of events that lead to plant senescence and the contribution of mitochondria to this process are largely unknown. This work is aimed to fill this gap by assessing the relative contribution of the mitochondria and cytosol of host cells to nodule aging.

Materials and Methods

Biological material

Common bean (*Phaseolus vulgaris* L. cv. Contender) seeds were surface sterilized with 70% ethanol, germinated in pots containing a 1:1 (v:v) mixture of perlite:vermiculite, inoculated 7 d later with *Rhizobium leguminosarum* bv *phaseoli* strain 3622, and grown on a nutrient solution containing 0.25 mM NH_4NO_3 in a controlled-environment chamber (Loscos *et al.,* 2008). Plants were separated randomly into three groups and nodules were harvested from plants at three different stages of development: young, *c.* 28-d-old plants without flowers; mature, *c.* 40-d-old plants at the late flowering-early fruiting stage; and senescent, *c.* 53-d-old plants with fully developed pods. Nodules were kept on ice and immediately used for purification of mitochondria and cytosol.

Purification of mitochondria and cytosol

All steps were performed at 0 to 4°C essentially as published (Iturbe-Ormaetxe *et al.*, 2001), with some modifications. Nodules (*c.* 10 g) were ground very gently in a mortar with 30 ml of a medium containing 0.35 M mannitol, 2 mM EDTA, 10 mM KH_2PO_4, 2% (w/v) polyvinylpoly-pyrrolidone and 30 mM morpholinepropanesulfonic acid (MOPS) (pH 7.2). The extract was filtered through four layers of cheesecloth and centrifuged twice at 4000*g* for 5 min. The supernatant was centrifuged at 12000*g* for 15 min and the pellet was saved. The soluble fraction was centrifuged at 50000*g* for 15 min and the new supernatant designated as 'cytosol'. The 12000*g* pellet was resuspended in 25 ml of washing medium consisting of 0.3 M mannitol, 1 mM EDTA and 20 mM MOPS (pH 7.2). After centrifugation at 12,000*g*, the pellet was resuspended in 1.8 ml of washing medium and carefully placed on top of a four-layer Percoll gradient. This was generated by centrifugation at 13000*g* for 35 min with a 70Ti rotor in an Optima XL-100K ultracentrifuge (Beckman Coulter, Fullerton, CA, USA). The mitochondria band, situated

between the 15% and 35% Percoll layers, was removed with a syringe. After two washes, mitochondria were resuspended in 500 µl of a medium containing 1 mM EDTA, 0.05% Triton X-100 and 50 mM MOPS (pH 7.2). For the MR, DR and GR assays, the resuspension medium was supplemented with 2 mM β-mercaptoethanol. For the GalLDH assay, the enzyme was extracted in a medium containing 50 mM Tris-HCl (pH 8.0) and 0.15% Triton X-100. Mitochondria were kept on ice for 1 h with occasional vortexing and then centrifuged at 13000*g* to remove intact organelles. Enzyme activities in the supernatant were assayed immediately. For proteomic and immunoblot analyses, the cytosolic and mitochondrial fractions were frozen at -80ºC.

Enzyme activity assays

SOD activity was assayed by a method based on the inhibition of cytochrome *c* reduction by superoxide at 550 nm (Rubio *et al.,* 2002). One SOD unit was defined as the amount of enzyme required to inhibit ferric cytochrome *c* reduction by 50%. APX and DR activities were determined following ascorbate oxidation at 290 nm (Asada, 1984) and ascorbate formation at 265 nm (Nakano & Asada, 1981), respectively. MR and GR activities were assayed by monitoring the oxidation of NADH (Dalton *et al.,* 1993) and NADPH (Dalton *et al.,* 1986) at 340 nm, respectively. GalLDH activity was determined following the reduction of cytochrome *c* at 550 nm as described (Matamoros *et al.,* 2006). All activities were assayed at 25ºC within the linear range. Glutamine synthetase (GS) activity was determined essentially as described in O'Neal & Joy (1973). Cytosol extracts were incubated for 5 min at 37°C in a buffer containing 20 mM $MgSO_4$, 1 mM diethylenetriaminepentaacetic acid, 80 mM glutamate, 6 mM NH_2OH, 8 mM ATP and 100 mM Tricine (pH 7.8). The reaction was terminated by addition of an equal amount of a solution containing 0.37 M $FeCl_3$, 0.67 M HCl and 0.2M trichloroacetic acid. The formation of γ-glutamyl hydroxamate was quantified spectrophotometrically at 540 nm using commercial γ-glutamyl hydroxamate as standard. Unless otherwise indicated, all activities were assayed at 25ºC within the linear range.

Protease activity

Endopeptidase activity was measured in the cytosol using azocasein as a substrate (Pfeiffer *et al.,* 1983). The cytosol fraction was isolated as described above, except that the extraction medium consisted of 0.35 M mannitol, 2 mM EDTA, 2% polyvinylpolypyrrolidone and 100 mM MES (pH 5.0). The cytosol (150 µl) was mixed with 250 µl azocasein (10 mg/ml in 50 mM Na-phosphate buffer, pH 7.0) and incubated at 37°C for 1 h. The reaction was stopped with 600 µl of 20% trichloroacetic acid, the samples were centrifuged at 13000*g* for 1 min, and 700 µl of supernatant was added to an equal amount of 1 M NaOH. In some experiments, cytosol extracts

were pre-incubated for 15 min at 37ºC with 100 μM of *trans*-epoxysuccinyl-L-leucylamido(4-guanidino)butane (E-64; Sigma–Aldrich) or 1 mM phenylmethylsulfonyl fluoride (PMSF; Sigma–Aldrich), which are specific inhibitors of cysteine proteinases and serine proteinases, respectively. One unit of endopeptidase activity was defined as the amount of enzyme required to produce a change in absorbance at 440 nm of 1.0 after 1 h.

Markers of senescence and oxidative stress

Lb concentration was determined by the pyridine-hemochrome assay (Appleby & Bergersen, 1980). The oxidative damage of lipids was measured by HPLC as malondialdehyde content after its reaction with thiobarbituric acid (Iturbe-Ormaetxe *et al.,* 1998). The oxidative damage of proteins was estimated as the content of total carbonyl groups. Proteins were separated on 12.5% SDS-gels, and carbonyls were quantified by derivatization with 2,4-dinitrophenylhydrazine using the OxyBlot Protein Oxidation Detection kit following the manufacturer's instructions (Chemicon, Temecula, CA, USA).

Gene expression analyses

These were carried out as described (Loscos *et al.,* 2008). In brief, RNA was isolated from bean nodules using the RNAqueous kit (Ambion) and treated with DNaseI (Roche) at 37ºC for 30 min. Equal amounts of genomic DNA-free RNA were used for cDNA synthesis with Moloney murine leukemia virus reverse transcriptase (Promega). Quantitative reverse transcription-PCR analyses were performed with the iCycler iQ instrument and iQ SYBR-Green Supermix reagent (Bio-Rad) using specific primers (Supporting Information Table S1). Four reference genes (*actin*, *protein phosphatase 2A subunit*, *ubiquitin* and *ubiquitin conjugating enzyme*) were initially used to normalize transcript levels. All but the *actin* gene showed stable expression during nodule aging. Values were used for normalization with *ubiquitin*, although expression patterns were confirmed with the reference genes *protein phosphatase 2A* and *ubiquitin conjugating enzyme*. The relative values of gene expression (R) were then calculated using the $2\exp(-\Delta\Delta C_T)$ method, where C_T is the threshold cycle (Livak & Schmittgen, 2001).

Immunoblot analyses

Cytosolic and mitochondrial proteins were separated on 15% SDS gels and transferred onto polyvinylidene fluoride membranes following standard protocols. Equal protein loading and transfer efficiency were assessed by Coomassie blue and Ponceau staining of gels and membranes, respectively. Immunoblot analyses were carried out using rabbit polyclonal antibodies against *Arabidopsis thaliana* mitochondrial PrxIIF (Finkemeier *et al.,* 2005) and

cytosolic PrxIIC (Horling *et al.,* 2003). Primary antibodies were used at a dilution of 1:1000, and the anti-rabbit IgG horseradish peroxidase conjugated secondary antibody at a dilution of 1:20000. Immunoreactive proteins were visualized using the SuperSignal West Pico (Pierce) chemiluminescent reagent.

Glutathione immunolocalization

Small pieces of nodules (1-2 mm^3) were fixed and embedded as described (Fernández-García *et al.,* 2009). Ultra-thin sections (80 nm) were obtained with a Leica EM UC6 ultramicrotome (Leica, Vienna, Austria) and collected on formvar-coated nickel grids. The grids were placed in phosphate-buffered saline (PBS) with 5% bovine serum albumin (BSA) for 30 min at room temperature and then incubated for 2 h with the primary antibody, anti-glutathione rabbit polyclonal IgG (Chemicon International, Temecula, CA, USA) diluted 1:50 in PBS containing 1% BSA plus 1% goat serum. The sections were washed three times in PBS and incubated for 1.5 h with the secondary antibody (goat anti-rabbit IgG coupled with 10 nm colloidal gold; British BioCell International, Cardiff, UK) diluted 1:50 in PBS supplemented with 1% BSA. The grids were washed in PBS and distilled water. Ultra-thin sections were stained with uranyl acetate followed by lead citrate. However, for better visualisation of differences in gold particle density, statistical evaluation was performed with cells from unstained sections. Negative controls were obtained by pre-adsorbing the anti-glutathione antibody with an excess of free glutathione prior to its application (Fernández-García *et al.,* 2009). Samples were viewed with a Tecnai 12 electron microscope (Philips, Eindhoven, The Netherlands) equipped with a CCD SIS MegaView III camera.

Morphometrical data were obtained as described by Fernández-García *et al.* (2009). Gold particle densities in the vacuoles and apoplast were very low (0.1 and 0.2 gold particles per μm^2, respectively), similar to the unspecific background labeling (0.2 gold particles per μm^2). The data obtained were analyzed statistically using Statistix 8 (NH Analytical Software, Roseville, MN, USA) and presented as the number of gold particles per μm^2.

Proteome and methionine sulfoxide analyses

Lyophilized mitochondrial and cytosolic fractions were resuspended in an ice-cold extraction buffer containing 25 mM MES (pH 7.2), 450 mM mannitol, 7 mM EDTA, 7 mM $CaCl_2$, 5 mM $MgCl_2$, 20 mM ascorbic acid and 10 mM dithiothreitol. Mitochondria were further broken and proteins resolubilized by sonication. Proteins were precipitated overnight at -20ºC after adding 20 vol of ice cold acetone containing 0.07% β-mercaptoethanol. Proteins were pelleted by centrifugation at 5000*g* for 20 min, washed with cold acetone and β-mercaptoethanol, and air

dried at room temperature. Dry pellets were resuspended in 8 M urea and 50 µg of protein was digested with 0.5 µg (1:100) of sequencing-grade endoproteinase Lys-C (Roche) for 5 h at 30ºC. For trypsin digestion, samples were diluted 1:4 in trypsin buffer (10% acetonitrile, 50 mM NH_4HCO_3, 2 mM $CaCl_2$). Fifty µg of protein was digested with 1.25 µl of trypsin beads (Applied Biosystems) at 37ºC overnight. Digested proteins were desalted using SPEC C_{18} columns (Agilent Technologies), and the resulting peptides were eluted with methanol, vacuum dried, and stored until use.

For proteomic analyses, samples were resuspended in 0.1% formic acid and 0.5 µg of protein sample was loaded onto a Peptide ES-18 column (15 cm x 0.1 mm, 2.7 µm; Sigma-Aldrich) in an Ultra HPLC Eksigent system (Axel Semrau, Sprockhövel, Germany) directly coupled to an Orbitrap XL mass spectrometer (Thermo Scientific, Rockford, IL, USA). Peptides were eluted with a 5% to 60% acetonitrile gradient for 100 min. Dynamic exclusion settings were as described (Hoehenwarter & Wienkoop, 2010). After mass spectrometry analysis, raw files were searched against the DFCI *Phaseolus vulgaris* Gene Index (v 4.0) using the Sequest algorithm. For identification and spectral count based data matrix generation, the Proteome Discoverer (v 1.2, Thermo Scientific) was used. A decoy database enabled false positive rate analysis. High confidence peptides (false positive rate <0.1%) with better than 3 ppm precursor mass accuracy and at least two distinct peptides per protein were considered to have passed the criteria. Dynamic modification was set for methionine oxidation. The peptide spectra information was stored in ProMEX (http://promex.pph.univie.ac.at/promex/). Five replicates per developmental stage and subfraction were analyzed. For relative protein quantification, changes in spectral counts of at least two-fold and $P \leq 0.05$ (*t*-test) were considered significant.

To determine the ratios of the methionine *versus* methionine sulfoxide (MetSO) peptide-containing species, the Mass Accuracy Precursor Alignment (MAPA; Hoehenwarter *et al.,* 2008) was used. In short, ion intensity counts for the precursor masses of the peptides were filtered using the ProtMAX software tool (Hoehenwarter *et al.,* 2008) and a data matrix was generated. The ratios between the oxidized *versus* the non-oxidized peptide species were calculated using their ion intensity counts (sum of precursor ion intensities for each target peptide).

Results

Oxidative stress occurs in mitochondria but not in the cytosol of senescing nodules

The involvement of mitochondria in nodule aging was assessed by isolating the cytosolic and mitochondrial fractions from bean nodules using differential centrifugation and Percoll density gradients. Nodules were harvested from plants at three different stages of development, termed ‘young’, ‘mature’ and ‘senescent’. To monitor nodule activity with advancing senescence, Lb, soluble protein and protease activity were quantified in the cytosol. Compared to young nodules, the concentrations of Lb and soluble protein in mature nodules did not vary significantly but decreased sharply in senescent nodules (Supporting Information Fig. S1a). Protease activity against azocasein was 4.5-fold greater in senescent nodules than in young or mature nodules (Fig. S1b). This protease activity was partly inhibited by phenylmethylsulfonyl fluoride, an inhibitor of serine proteinases, but not by E64, an inhibitor of cysteine proteinases (Fig. S1b).

The contribution of oxidative stress to the loss of nodule activity was investigated in the mitochondria and cytosol using lipid peroxidation (malondialdehyde) and protein oxidation (carbonyl groups) as markers (Halliwell & Gutteridge, 2007). Compared to young nodules, in mitochondria isolated from mature and senescent nodules, the amount of lipid peroxides increased by 48% and 75%, respectively (Fig. 1a), and the corresponding increases in oxidized proteins were 87% and 3.3-fold (Fig. 1b). By contrast, lipid peroxides in the cytosol of mature nodules decreased by 40% relative to young nodules (Fig. 1a) and the amount of oxidized proteins remained constant (Fig. 1b). Therefore, the mitochondria, but not the cytosol, experience oxidative stress during nodule aging.

Ascorbate and (homo)glutathione metabolism is impaired in senescing nodule mitochondria

Because oxidative modifications of lipids and proteins were preferentially detected in senescing nodule mitochondria and these alterations might have originated from an inadequate antioxidant protection, we compared some important antioxidant enzymes and metabolites in the mitochondria and cytosol. Mitochondria of leaves (Jiménez *et al.,* 1998) and nodules (Iturbe-Ormaetxe *et al.,* 2001) contain a functional ascorbate-glutathione pathway in which four enzyme activities, acting in concert, keep H_2O_2 under control using NAD(P)H as reductant. In bean nodule mitochondria, APX and GR activities remained unaltered during senescence (Fig. 2a). However, MR activity was reduced by 49% at the senescent stage, whereas DR activity declined by 15% in mitochondria of mature and senescent nodules (Fig. 2a). In contrast, the activities of MR, DR and GR in the cytosol either increased or remained stable with advancing age, whereas cytosolic APX activity declined by 30% (Fig. 2b). To complete this part of the study, we attempted to estimate indirectly the effect of senescence on ascorbate and (homo)glutathione concentrations in nodule mitochondria. A direct quantification was not reliable because the concentrations are low and the isolation of mitochondria using differential centrifugations and Percoll gradients may cause leakage of water-soluble metabolites. Thus, to get an indication of ascorbate metabolism, we measured GalLDH activity, a mitochondrial enzyme that catalyzes the last step of ascorbate biosynthesis (Wheeler *et al.,* 1998). This activity decreased by 30% in senescing nodules (data not shown), providing support for a limitation of ascorbate synthesis in mitochondria. On the other hand, an attempt was made to immunolocalize and quantify homoglutathione, the thiol tripeptide that replaces glutathione in bean nodules (Matamoros *et al.,* 1999b). The antibody raised against glutathione recognized both the reduced and oxidized (disulfide) forms (Fernández-García *et al.,* 2009) but, unfortunately, did not recognize

homoglutathione. We thus decided to quantify total glutathione (reduced + oxidized) in the mitochondria and cytosol of pea (*Pisum sativum*) nodules (Fig. 3, Table 1), on the assumption that the relative abundance and response of the thiol during aging in the two cellular compartments are similar in bean and pea nodules. This is supported by the observations that in both types of nodules there is a progressive decrease in thiols during senescence induced by nitrate (Escuredo *et al.,* 1996) or prolonged darkness of plants (Gogorcena *et al.,* 1997). Another advantage is that pea nodules contain high concentrations of glutathione, which facilitates immunolocalization. Gold particles, marking the presence of glutathione, were observed (Fig. 3a-c) and counted (Table 1) in the mitochondria, cytosol, nuclei and bacteroids of infected cells. There was also weak labeling in the peroxisomes and plastids (data not shown). In young nodules, glutathione concentration was similar in the mitochondria and cytosol, whereas in mature nodules labeling was five-fold more abundant in the cytosol than in the mitochondria. In senescent nodules, labeling virtually disappeared in the mitochondria and cytosol (Table 1). Labeling in the bacteroids was much more intense than in the other cell compartments, and was highest in mature nodules and drastically reduced in senescent nodules (Fig. 3a, Table 1). Interestingly, significant labeling was also observed in the nucleus of infected cells (Fig. 3c), which is in agreement with the recent detection of glutathione in the nuclei of leaf cells (Fernández-García *et al.,* 2009) or cultured cells (Diaz Vivancos *et al.,* 2010) of *A. thaliana*. As was the case for the cytosol and bacteroids, labeling intensity in the nuclei was maximal in mature nodules and consistently declined in senescent nodules (Table 1).

Mitochondrial MnSOD and alternative oxidase are upregulated during nodule aging

The effects of nodule aging on two other key antioxidants of plant mitochondria, SOD and alternative oxidase (AOX), were also examined (Fig. 4). Mitochondrial MnSOD is

located in the matrix and catalyzes the dismutation of O_2^- to H_2O_2, whereas AOX is located in the membrane and may participate in the protection of plant mitochondria from high ROS levels due to its ability to catalyze non-coupled respiratory electron transport (Vanlerberghe *et al.,* 2009). The activity of MnSOD increased by 36% and >50% in mature and senescent nodules, respectively (Fig. 4a). Likewise, the AOX transcript level was 13-fold higher in senescent nodules than in young nodules (Fig. 4b). These findings may reflect enhanced generation of O_2^- with age as a result of electron leakage from the respìratory chain (Rhoads *et al.,* 2006).

The Trx-Prx redox system may be compromised in aging nodules

The cytosol and mitochondria of legume nodules contain Trx-Prx redox systems that catalyze the reduction of H_2O_2 and other hydroperoxides (Tovar-Méndez *et al.,* 2011). The mRNA levels of mitochondrial Trx*o* and PrxIIF declined significantly during nodule aging (Fig. 5). However, immunoblot analysis (Fig. S1c) revealed that the content of PrxIIF protein remained constant. Therefore, the enzyme is apparently quite stable and has a low turnover rate. Immunoblot analyses under non-reducing conditions indicated that the protein is present as high molecular mass aggregates, suggesting that PrxIIF is able to form oligomers or heterocomplexes with other proteins *in vivo*. The nodule cytosol also contains a NTR-Trx-Prx system comprising several NTR and Trx*h* isoforms and PrxIIB/C. The most abundant Trx isoforms in *L. japonicus* nodules are Trx*h1* and Trx*h4* (Tovar-Méndez *et al.,* 2011). Interestingly, the bean Trx*h4* isoform investigated here is probably the functional equivalent of a soybean Trx*h* essential for ROS scavenging in nodules (Lee *et al.,* 2005). Nodule aging led to significant decreases of PrxIIB mRNA and protein levels and of the Trx*h4* mRNA level, whereas no effect was seen on the Trx*h1* transcript (Fig. 5, Fig. S1c).

Mitochondrial and cytosolic proteomes

Proteomics is a powerful tool to investigate metabolic pathways in various tissues and stressful conditions. The effect of aging on the mitochondrial proteome, however, has not yet been reported in plants. Here, 143 proteins of mitochondria and 81 proteins of the cytosol were identified with high stringency and functionally classified.

The enzymes involved in the tricarboxylic acid cycle and oxidative phosphorylation accounted for the largest functional group in nodule mitochondria, but proteins related to amino acid metabolism, nucleotide metabolism and ureide biosynthesis were also widely represented (Table 2). In addition, the detection in mitochondrial extracts of catalase and glutamate synthase, marker enzymes of peroxisomes and plastids, respectively, indicates some contamination of mitochondria preparations with these organelles. To estimate protein abundance, a normalization similar to the Protein Abundance Index (Rappsilver *et al.,* 2002) was used. The total spectral counts were normalized for catalase and the mitochondrial ATPase β-subunit, which have similar molecular masses (*c.* 60 kDa). This comparison revealed that the abundance of the mitochondrial protein is at least 10-fold greater than that of catalase. Also, the ratio of cytocrome *c* oxidase to uricase activity, which is an indicator of mitochondria purity with respect to peroxisomes, was 37-fold higher in purified mitochondria than in whole nodule extracts (Iturbe-Ormaetxe *et al.*, 2001). On the other hand, glutamate synthase is a large sized plastidic enzyme (*c.* 240 kDa) and therefore a direct comparison of the relative abundance of glutamate synthase and the ATPase β–subunit is only possible after normalization. This comparison showed that the abundance of glutamate synthase is *c.* 600-fold lower than that of ATPase. Overall, our results indicate that mitochondria showed a low contamination with peroxisomes and plastids.

The effect of aging was less pronounced on the mitochondrial proteome than on the cytosolic proteome. Thus, 28% of the mitochondrial proteins (Table 2) and 63% of the

cytosolic proteins (Table 3) identified in this work showed decreased levels in aged nodules. In mitochondria, proteins that are crucial for nitrogen and carbon metabolism (glutamate dehydrogenase and aspartate aminotransferase) or that are involved in the recognition and translocation of mitochondrial preproteins (TOM20) decreased in senescent mitochondria (Table 2). Only two proteins of mitochondria from senescent nodules were induced with aging, a hypersensitive response induced protein and a carboxylesterase. The decrease in cytosolic proteins was particularly intense for proteins related to protein synthesis and cytoskeleton organization (Table 3). Notably, some actin and β-tubulins were already reduced in mature nodules, which suggests that the disorganization of cytoskeletal structures is an early event during aging of nodule host cells. The contents of phospho*enol*pyruvate carboxylase and CuZnSOD decreased in mature and senescent nodules. Only one protein, heme oxygenase, which is involved in heme catabolism, was induced in mature and senescent nodules with respect to young nodules.

Post-translational modifications of mitochondrial and cytosolic proteins

The free radical NO is a major signal molecule that participates in many crucial processes of plants (Lamotte *et al.,* 2005). In nodules, NO is a key player in the onset of symbiosis (Baudouin *et al.,* 2006; del Giudice *et al.,* 2011) and in senescence (Cam *et al.,* 2012). Unregulated production of NO may result, however, in formation of peroxynitrite and other nitrating species leading to nitrosative stress (Valderrama *et al.,* 2007; Corpas *et al.,* 2011). We investigated if aging leads to the accumulation of nitrated proteins in the mitochondria and cytosol. To this end, we used an antibody against nitro-tyrosine because increased levels of this compound have been found in plant tissues exposed to abiotic stress (Corpas *et al.,* 2011). Contrary to our expectations, nodule aging was accompanied by a decline in cytosolic and mitochondrial proteins containing nitro-tyrosine, which indicates that nitrosative stress was not involved.

On the other hand, the oxidation of methionine to MetSO and the reduction of MetSO back to methionine by peptide MetSO reductases are emerging as a novel mechanism for regulation of cell function (Hardin *et al.,* 2009). Using proteomic analysis combined with the targeted MAPA approach (see Materials & Methods) we found that the MetSO content in mitochondrial or cytosolic proteins did not increase with aging, with the exception of nodulin 6l and glutamine synthetase (GS). The effect of methionine oxidation on GS activity was studied in more detail as this enzyme is essential for controlling carbon and nitrogen metabolism in nodules (Vance, 2008) and has been recently found to be also a target of tyrosine nitration (Melo *et al.,* 2011). The GS-N1 isoform contains two methionine residues at positions 31 and 33 that are oxidized to MetSO during aging (Fig. 6). However, methionine oxidation could not be detected in GS-PR1, another cytosolic isoform, in agreement with the observation that in this protein leucine substitutes for the two methionine residues susceptible to oxidation. The effect of methionine sulfoxidation on GS activity was examined in the cytosol of young, mature and senescent nodules. However, no significant differences could be observed in the total GS activity (GS-N1 + GS-PR1), which may be explained either by a genuine lack of effect of sulfoxidation on GS-N1 activity or by a masking effect of GS-PR1 activity, which does not bear MetSO.

Discussion

Legume nodule senescence is a poorly understood process that begins early after the onset of pod filling (Bethlenfalvay & Phillips, 1977) and is characterized by a decrease in N_2 fixation, Lb and total protein and by a concomitant increase in protease activity (Pladys & Vance, 1993; Puppo *et al.,* 2005; Groten *et al.,* 2006; Loscos *et al.,* 2008). In this work, most of these changes were monitored as markers of nodule senescence. Two novel observations concerning Lb and proteases are noteworthy. First, the induction of

heme oxygenase, an enzyme catalyzing the oxidation of heme to carbon monoxide, free iron and biliverdins (Shekhawat & Verma, 2010). This induction is probably associated with the decrease in Lb (Fig. S1) and the increase in biliverdin-like pigments that are present in the extracts of senescent nodules (data not shown). The release of free heme from Lb, which may be favored by high proteolytic activity and acidic conditions in senescent nodules, could induce heme oxygenase, although the induction of heme oxygenase genes by heme is still controversial in plants (Baudouin *et al.,* 2004). Second, our experiments with protease inhibitors suggest that the endoprotease activity in the cytosol of senescent bean nodules is mainly due to serine proteinases rather than cysteine proteinases, which is at odds with the situation described in senescing alfalfa (*Medicago sativa*) nodules (Pladys & Vance, 1993). Compartmentalization of some cysteine proteinases in the vacuoles or symbiosomes, as suggested by Pérez-Guerra *et al.* (2010), could explain the differences because the experiments in alfalfa were carried out in whole nodule extracts whereas we used purified cytosol. Groten *et al.* (2006) reported increases in cysteine and serine proteinase activities during aging of pea nodules, pointing to interspecific variations in the major types of proteases associated with senescence.

A proteomic approach was used also to investigate the changes in protein levels of the mitochondria and cytosol during the natural senescence of nodules. This type of study is innovative and important because no data are available so far on the proteomes of both nodule sub-fractions. Proteomic analysis revealed that nodule aging entails a marked decline in the concentration of nearly all cytosolic proteins, which can be largely attributed to enhanced proteolytic activity. These data also indicated that some key proteins for nodule function, such as phospho*enol*pyruvate carboxylase, CuZnSOD and proteins involved in cytoskeleton dynamics and protein synthesis, were already compromised at the mature stage, prior to any evident symptom of senescence. However, the number of mitochondrial proteins showing reduced levels in senescent nodules was considerably lower than that of the corresponding cytosolic proteins. In mitochondria, the

major decreases were observed for the enzymes of *de novo* purine biosynthetic pathway. These results are consistent with lower rates of N_2 fixation in senescent nodules because purines are precursors of ureides, the form in which nitrogen is transported from nodules to the shoot in tropical legumes (Vance, 2008).

Oxidative stress is frequently associated with plant senescence. Elevated levels of randomly oxidized molecules cause cell dysfunction and ultimately cell death. Nevertheless, specific oxidation of key cell components may afford redox signals ('oxidative signaling') that can be involved in the orchestration of senescence (Foyer & Noctor, 2005). The occurrence of oxidative stress in aging nodules has been reported in soybean (Evans *et al.,* 1999), lupin (*Lupinus albus*; Hernández-Jiménez *et al.,* 2002) and bean (Loscos *et al.,* 2008), but not in pea (Groten *et al.,* 2005). In all these studies whole nodules were analyzed, which provides only partial information and possibly overlooks oxidative events localized in organelles. Here we present new data about the effects of natural senescence on the major antioxidants of nodule mitochondria. Specifically, our results underline the importance of ascorbate and glutathione in nodule senescence at the subcellular level. Changes in the concentrations and redox states of both antioxidants are inherent to nodule senescence (Evans *et al.,* 1999; Matamoros *et al.,* 1999a; Groten *et al.,* 2005; Vanacker *et al.,* 2006; Loscos *et al.,* 2008). We show that aging reduced the capacity of mitochondria, but not of the cytosol, to regenerate ascorbate. Also, the immunological approach used in this work allowed the first direct quantification of glutathione in nodule organelles. The early decrease of glutathione in mitochondria from mature nodules is remarkable and may be due to transport and/or degradation but not to the inhibition of thiol synthesis, which only occurs in the cytosol and plastids (Clemente *et al.,* 2012). Therefore, the redistribution of glutathione and its subsequent effects on the mitochondrial redox state appear to be important features of nodule senescence. Interestingly, Diaz Vivancos *et al.* (2010) found that cytosolic glutathione is recruited in the nuclei during cell proliferation. However, because in the present work the relative

levels of glutathione were quantified in infected cells rather than in meristematic, actively dividing cells of pea nodules, glutathione should perform additional functions in the nuclei, probably related to the redox regulation of transcription factors and the protection of DNA against oxidative damage. In mitochondria, the decrease of glutathione and probably of ascorbate, as a result of diminished MR, DR and GalLDH activities, may trigger an oxidative state during senescence, as evidenced by the accumulation of lipid peroxides and carbonylated proteins. The induction of MnSOD and AOX reflects an increased generation of ROS during electron transport and likely contributes to the oxidative state of senescing mitochondria.

The high levels of oxidized proteins in mitochondria of senescing nodules were accompanied only by moderate proteolysis in comparison to the cytosol, according to proteomic analyses. Conversely, the high proteolytic activities in the cytosol were not accompanied by increases in oxidized proteins. These findings are novel and unexpected because oxidized proteins have been reported to be more susceptible to degradation (Palma *et al.,* 2002). Two explanations are that mitochondrial proteases are not fully proficient in removing oxidized proteins and that protein carbonylation is a selective process yielding modified proteins with useful functions. In humans, moderately damaged proteins are prone to attack by proteases, but extensively damaged proteins may be more resistant and tend to form aggregates (Møller & Kristensen, 2004).

On the other hand, peptides derived from mitochondrial oxidized proteins could act as secondary messengers and participate in retrograde ROS signaling (Møller & Sweetlove, 2010). Nevertheless, the mechanism by which ROS derived from mitochondria influences cell metabolism is unknown. The identification of oxidatively modified proteins with altered activities is crucial to understand how cells respond and adapt to redox changes. Our proteomic analysis, combined with the use of cutting-edge methodology capable of detecting peptides differing only in the presence of MetSO (Hoehenwarter *et al.,* 2008), revealed that specific methionine residues of a cytosolic GS

isoform (GS-N1) are sulfoxidized in mature and senescent nodules. The post-translational inactivation of GS by tyrosine nitration has been reported (Melo *et al.,* 2011). These authors proposed that GS inactivation is related to the inhibition of nitrogenase by NO, thus establishing a direct link between N_2 fixation and ammonia assimilation in nodules. We report here, for the first time, that methionine sulfoxidation is also important for the regulation of GS in response to ROS. Taking together all these findings, we propose that cytosolic GS is a central element in the cellular signaling network in nodules.

In conclusion, our results provide evidence that changes in the concentration of ascorbate and glutathione and in the capacity to regenerate ascorbate during nodule senescence induce an oxidative shift in mitochondria, which is consistent with the upregulation of MnSOD and AOX. This oxidative state is evidenced by the accumulation of oxidized lipids and proteins, which may be acting also as signaling molecules. Senescence is accompanied by a reduction of key enzymes implicated in carbon metabolism, by the disorganization of the cytoskeleton, and by a sharp and general reduction of cytosolic proteins due to inhibition of protein synthesis and induction of proteolytic activity.

Supporting Information

Additional supporting information may be found in the online version of this article.

Fig. S1 (a) Protein and leghemoglobin (Lb) contents, (b) protease activity against azocasein in the cytosol, and (c) immunoblots of mitochondrial peroxiredoxin PrxIIF and cytosolic peroxiredoxin PrxIIB/C in young (Y), mature (M) and senescent (S) bean nodules.

In (b) the effects of the inhibitors of cysteine proteinase (E64) and serine proteinase (phenylmethylsulfonyl fluoride, PMSF) are shown. In (a) and (b) values are means ± SE of four replicates, and means denoted by the same letter are not significantly different at $P<0.05$ based on Duncan's multiple range test. In (c) gels were loaded with 10 µg (PrxIIF) or 40 µg (PrxIIB/C) of protein per lane. The apparent molecular masses in both cases were 19 kDa. Blots are representative of three to five gels loaded with extracts from different plants.

Acknowledgements

We thank Carmen Pérez-Rontomé for assistance with growing the plants and drawing the figures, Christiana Staudinger for help with proteomic analyses, Enrique Olmos and Euan James for valuable comments on glutathione immunolocalization, and Frank Minchin and two anonymous reviewers for constructive criticism on the manuscript. This work was funded by Ministerio de Ciencia e Innovación-Fondo Europeo de Desarrollo Regional (AGL2011-24524) and Gobierno de Aragón-Fondo Social Europeo (group A53).

References

Appleby CA, Bergersen FJ. 1980. Preparation and experimental use of leghemoglobin. *In* FJ Bergersen, ed, Methods for Evaluating Biological Nitrogen Fixation. John Wiley, Chichester, UK, pp 315–335.

Asada K. **1984.** Chloroplasts, formation of active oxygen and its scavenging. *Methods in Enzymology* **105:** 422-429.

Baudouin E, Pieuchot L, Engler G, Pauly N, Puppo A. 2006. Nitric oxide is formed in *Medicago truncatula-Sinorhizobium meliloti* functional nodules. *Molecular Plant Microbe-Interactions* **19:** 970–975.

Bethlenfalvay GJ, Phillips DA. 1977. Ontogenetic interactions between photosynthesis and symbiotic nitrogen fixation in legumes. *Plant Physiology* **60:** 419–421.

Cam Y, Pierre O, Boncompagni E, Hérouart D, Meilhoc E, Bruand C. 2012. Nitric oxide (NO): a key player in the senescence of *Medicago truncatula* root nodules. *New Phytologist* **196:** 548-560.

Clemente MR, Bustos-Sanmamed P, Loscos J, James EK, Pérez-Rontomé C, Navascués J, Gay M, Becana M. 2012. Thiol synthetases of legumes: immunogold localization and differential gene regulation by phytohormones. *Journal of Experimental Botany* **63:** 3923-3934.

Corpas FL, Leterrier M, Valderrama R, Airaki M, Chaki M, Palma JM, Barroso JB. 2011. Nitric oxide imbalance provokes a nitrosative response in plants under abiotic stress. *Plant Science* **181:** 604-611.

Dalton DA, Baird LM, Langeberg L, Taugher CY, Anyan WR, Vance CP, Sarath G. 1993. Subcellular localization of oxygen defense enzymes in soybean (*Glycine max* [L.] Merr.) root

nodules. *Plant Physiology* **102:** 481–489.

Dalton DA, Russell SA, Hanus FJ, Pascoe GA, Evans HJ. 1986. Enzymatic reactions of ascorbate and glutathione that prevent peroxide damage in soybean root nodules. *Proceedings of the National Academy of Sciences, USA* **83:** 3811–3815.

del Giudice J, Cam Y, Damiani I, Fung-Chat F, Meilhoc E, Bruand C, Brouquisse R, Puppo A, Boscari A. 2011. Nitric oxide is required for an optimal establishment of the *Medicago truncatula–Sinorhizobium meliloti* symbiosis. *New Phytologist* **191:** 405–417.

Diaz Vivancos P, Dong Y, Ziegler K, Markovic J, Pallardó FV, Pellny TK, Verrier PJ, Foyer CH. 2010. Recruitment of glutathione into the nucleus during cell proliferation adjusts whole-cell redox homeostasis in *Arabidopsis thaliana* and lowers the oxidative defence shield. *Plant Journal* **64:** 825–838.

Dietz K-J, Jacob S, Oelze M-L, Laxa M, Tognetti V, Nunes de Miranda MS, Baier M, Finkemeier I. 2006. The function of peroxiredoxins in plant organelle redox metabolism. *Journal of Experimental Botany* **57:** 1697–1709.

Escuredo PR, Minchin FR, Gogorcena Y, Iturbe-Ormaetxe I, Klucas RV, Becana M. 1996. Involvement of activated oxygen in nitrate-induced senescence of pea root nodules. *Plant Physiology* **110:** 1187-1195.

Evans PJ, Gallesi D, Mathieu C, HernándezMJ, de Felipe M, Halliwell B, Puppo A. 1999. Oxidative stress occurs during soybean nodule senescence. *Planta* **208:** 73–79.

Fernández-García N, Martí MC, Jiménez A, Sevilla F, Olmos E. 2009. Sub-cellular distribution of glutathione in an Arabidopsis mutant (*vtc1*) deficient in ascorbate. *Journal of Plant Physiology* **166:** 2004-2012.

Finkemeier I, Goodman M, Lamkemeyer P, Kandlbinder A, Sweetlove LJ, Dietz KJ. 2005. The mitochondrial type II peroxiredoxin F is essential for redox homeostasis and root growth of Arabidopsis thaliana under stress. *Journal of Biological Chemistry* **280:** 12168–12180.

Foyer CH, Noctor G. 2005. Oxidant and antioxidant signalling in plants: a re-evaluation of the concept of oxidative stress in a physiological context. *Plant Cell & Environment* **28:** 1056-1071.

Gogorcena Y, Gordon AJ, Escuredo PR, Minchin FR, Witty JF, Moran JF, Becana M. 1997. N_2 fixation, carbon metabolism, and oxidative damage in nodules of dark-stressed common bean plants. *Plant Physiology* **113:** 1193-1201.

Groten K, Vanacker H, Dutilleul C, Bastian F, Bernard S, Carzaniga R, Foyer CH. 2005. The roles of redox processes in pea nodule development and senescence. *Plant Cell & Environment* **28:** 1293–1304.

Groten K, Dutilleul C, van Heerden PD, Vanacker H, Bernard S, Finkemeier I, Dietz KJ,

Foyer CH. 2006. Redox regulation of peroxiredoxin and proteinases by ascorbate and thiols during pea root nodule senescence. *FEBS Letters* **580:** 1269–1276.

Halliwell B, Gutteridge JMC. 2007. *Free radicals in biology and medicine, 4th edn*. Oxford, UK: Oxford University Press.

Hardin SC, Larue CT, Oh MH, Jain V, Huber SC. 2009. Coupling oxidative signals to protein phosphorylation via methionine oxidation in *Arabidopsis*. *Biochemical Journal* **422:** 305-312.

Hernández-Jiménez MJ, Lucas MM, de Felipe MR. 2002. Antioxidant defence and damage in senescing lupin nodules. *Plant Physiology and Biochemistry* **40:** 645–657.

Hoehenwarter W, van Dongen JT, Wienkoop S, Steinfath M, Hummel J, Erban A, Sulpice R, Regierer B, Kopka J, Geigenberger P, *et al.* 2008. A rapid approach for phenotype-screening and database independent detection of cSNP/protein polymorphism using mass accuracy precursor alignment. *Proteomics* **8**: 4214-4225.

Hoehenwarter W, Wienkoop S. 2010. Spectral counting robust on high mass accuracy mass spectrometers. *Rapid Communications in Mass Spectrometry* **24:** 3609–3614.

Horling F, Lamkemeyer P, König J, Finkemeier I, Kandlbinder A, Baier M, Dietz KJ. 2003. Divergent light-, ascorbate-, and oxidative stress-dependent regulation of expression of the peroxiredoxin gene family in Arabidopsis. *Plant Physiology* **131:** 317–325.

Iturbe-Ormaetxe I, Escuredo PR, Arrese-Igor C, Becana M. 1998. Oxidative damage in pea plants exposed to water deficit or paraquat. *Plant Physiology* **116:** 173-181.

Iturbe-Ormaetxe I, Matamoros MA, Rubio MC, Dalton DA, Becana M. 2001. The antioxidants of legume nodule mitochondria. *Molecular Plant-Microbe Interactions* **14:** 1189-1196.

Jiménez A, Hernández JA, Pastori GM, del Río LA, Sevilla F. 1998. Role of the ascorbate–glutathione cycle of mitochondria and peroxisomes in the senescence of pea leaves. *Plant Physiology* 118: 1327–1335.

Laloi C, Rayapuram N, Chartier Y, Grienenberger JM, Bonnard G, Meyer Y. 2001. Identification and characterization of a mitochondrial thioredoxin system in plants. *Proceedings of the National Academy of Sciences, USA* **98:** 14144–14149.

Lamotte L, Courtois C, Barnavon L, Pugin A, Wendehenne D. 2005. Nitric oxide in plants: the biosynthesis and cell signalling properties of a fascinating molecule. *Planta* **221:** 1–4.

Lim PO, Kim HJ, Nam HG. 2007. Leaf senescence. *Annual Review of Plant Biology* **58:** 115–36.

Lee MY, Shin KH, Kim YK, Suh JY, Gu YY, Kim MR, Hur YS, Son O, Kim JS, Song E, *et al.* 2005. Induction of thioredoxin is required for nodule development to reduce reactive oxygen species levels in soybean roots. *Plant Physiology* **139:** 1881–1889.

Livak KJ, Schmittgen TD. 2001. Analysis of relative gene expression data using real-time quantitative PCR and the 2-DCt method. *Methods* **25:** 402–408.

Loscos J, Matamoros MA, Becana M. 2008. Ascorbate and homoglutathione metabolism in common bean nodules under stress conditions and during natural senescence. *Plant Physiology* **146:** 1282–1292.

Matamoros MA, Baird LM, Escuredo PR, Dalton DA, Minchin FR, Iturbe-Ormaetxe I, Rubio MC, Moran JF, Gordon AJ, Becana M. 1999a. Stress induced legume root nodule senescence: physiological, biochemical, and structural alterations. *Plant Physiology* **121:** 97–111.

Matamoros MA, Moran JF, Iturbe-Ormaetxe I, Rubio MC, Becana M. 1999b. Glutathione and homoglutathione synthesis in legume root nodules. *Plant Physiology* **121:** 879–888.

Matamoros MA, Loscos J, Coronado MJ, Ramos J, Sato S, Testillano PS, Tabata S, Becana M. 2006. Biosynthesis of ascorbic acid in legume root nodules. *Plant Physiology* **141:** 1068–1077.

Maxwell DP, Nickels R, McIntosh L. 2002. Evidence of mitochondrial involvement in the transduction of signals required for the induction of genes associated with pathogen attack and senescence. *Plant Journal* **29:** 269–279.

Melo PM, Silva LS, Ribeiro I, Seabra AR, Carvalho HG. 2011. Glutamine synthetase is a molecular target of nitric oxide in root nodules of *Medicago truncatula* and is regulated by tyrosine nitration. *Plant Physiology* **157:** 1505–1517.

Møller IM, Kristensen BK. 2004. Protein oxidation in plant mitochondria as a stress indicator. *Photochemical & Photobiological Sciences* **3:** 730-735.

Møller IM, Sweetlove LJ. 2010. ROS signalling – specificity is required. *Trends in Plant Science* **15:** 370–374.

Nakano Y, Asada K. 1981. Hydrogen peroxide is scavenged by ascorbate specific peroxidase is spinach chloroplasts. *Plant and Cell Physiology* **22:** 867-880.

Noctor G, De Paepe R, Foyer CH. 2007. Mitochondrial redox biology and homeostasis in plants. *Trends in Plant Science* **12:** 125–134.

Oldroyd GED, Downie JA. **2008.** Coordinating nodule morphogenesis with rhizobial infection in legumes. *Annual Review of Plant Biology* **59:** 519–546.

O'Neal D, Joy KW. 1973. Glutamine synthetase of pea leaves. Purification, stabilization, and pH optima. *Archives of Biochemistry and Biophysics* **159:** 113-122.

Palma JM, Sandalio LM, Corpas FJ, Romero-Puertas MC, McCarthy I, del Río LA. 2002. Plant proteases, protein degradation, and oxidative stress: role of peroxisomes. *Plant Physiology Biochemistry* **40:** 521-530.

Palma JM, Jiménez A, Sandalio LM, Corpas FJ, Lundqvist M, Gómez M, Sevilla F, del Río LA. 2006. Antioxidative enzymes from chloroplasts, mitochondria, and peroxisomes during leaf senescence of nodulated pea plants. *Journal of Experimental Botany* **57:** 1747–1758.

Pérez-Guerra JC, Coussens G, De Keyser A, De Rycke R, De Bodt S, Van De Velde W, Goormachtig S, Holsters M. 2010. Comparison of developmental and stress-induced nodule senescence in *Medicago truncatula*. *Plant Physiology* **152:** 574–1584.

Pfeiffer NE, Torres CM, Wagner FW. 1983. Proteolytic activity in soybean root nodules. *Plant Physiology* **71:** 797-802.

Pladys D, Vance CP. 1993. Proteolysis during development and senescence of effective and plant gene-controlled ineffective alfalfa nodules. *Plant Physiology* **103:** 379-384.

Puppo A, Groten K, Bastian F, Carzaniga R, Soussi M, Lucas MM, De Felipe MR, Harrison J, Vanacker H, Foyer CH. 2005. Legume nodule senescence: roles for redox and hormone signalling in the orchestration of the natural aging process. *New Phytologist* **165:** 683–701.

Rappsilber J, Ryder U, Lamond AI, Mann M. 2002. Large-scale proteomic analysis of the human spliceosome. *Genome Research* **12:** 1231–1245.

Rhoads DM, Umbach AL, Subbaiah CC, Siedow JN. 2006. Mitochondrial reactive oxygen species. Contribution to oxidative stress and interorganellar signalling. *Plant Physiology* **141:** 357–366.

Rubio MC, González EM, Minchin FR, Webb KJ, Arrese-Igor C, Ramos J, Becana M. 2002. Effects of water stress on antioxidant enzymes of leaves and nodules of transgenic alfalfa overexpressing superoxide dismutases. *Physiologia Plantarum* **115:** 531–540.

Rubio MC, James EK, Clemente MR, Bucciarelli B, Fedorova M, Vance CP, Becana M. 2004. Localization of superoxide dismutases and hydrogen peroxide in legumeroot nodules. *Molecular Plant-Microbe Interactions* **17:** 1294-1305.

Schriner SE, Linford NJ, Martin GM, Treuting P, Ogburn CE, Emond M, Coskun PE, Ladiges W, Wolf N, Van Remmen H, Wallace DC, Rabinovitch PS. **2005.** Extension of murine life span by overexpression of catalase targeted to mitochondria. *Science* **308:** 1909-1911.

Shekhawat GS, Verma K. 2010. Haem oxygenase (HO): an overlooked enzyme of plant metabolism and defence. *Journal of Experimental Botany* **61:** 2255-2270.

Tovar-Méndez A, Matamoros MA, Bustos-Sanmamed P, Dietz K-J, Cejudo FJ, Rouhier N, Sato S, Tabata S, Becana M. 2011. Peroxiredoxins and NADPH-dependent thioredoxin systems in the model legume *Lotus japonicus*. *Plant Physiology* **156:** 1535–1547.

Valderrama R, Corpas FJ, Carreras A, Fernández-Ocaña A, Chaki M, Luque F, Gómez-Rodríguez MV, Colmenero-Varea P, del Río LA, Barroso JB. 2007. Nitrosative stress in

plants. *FEBS Letters* **581:** 453-461.

Vanacker H, Sandalio LM, Jiménez A, Palma JM, Corpas FJ, Meseguer V, Gómez M, Sevilla F, Leterrier M, Foyer CH, *et al.* 2006. Roles for redox regulation in leaf senescence of pea plants grown on different sources of nitrogen nutrition. *Journal of Experimental Botany* **57:** 1735–1745.

Vance CP. 2008. Carbon and nitrogen metabolism in legumes nodules. *In* MJ Dilworth *et al.* eds, Nitrogen-fixing Leguminous Symbioses, pp 293–320.

Vanlerberghe GC, Cvetkovska M, Wang J. 2009. Is the maintenance of homeostatic mitochondrial signaling during stress a physiological role for alternative oxidase? *Physiologia Plantarum* **137:** 392–406.

Wheeler GL, Jones MA, Smirnoff N. 1998. The biosynthetic pathway of vitamin C in higher plants. *Nature* **393:** 365–369.

Legends for Figures

Fig. 1 (a) Lipid peroxidation and (b) protein carbonylation in mitochondria and cytosol of young (Y), mature (M) and senescent (S) bean nodules. Values are means ± SE of four to eight replicates, each from nodules of 15 plants. Means denoted by the same letter are not significantly different at $P<0.05$ based on Duncan's multiple range test. MDA, malondialdehyde.

Fig. 2 Specific activities of the enzyme of the ascorbate-(homo)glutathione pathway in (a) mitochondria and (b) cytosol of young (Y), mature (M) and senescent (S) bean nodules. Values are means ± SE of four to eight replicates, each from nodules of 15 plants. Means denoted by the same letter are not significantly different at $P<0.05$ based on Duncan's multiple range test.

Fig. 3 Immunogold localization of glutathione in pea nodules. Images show intense labeling in (a) bacteroids of a mature nodule, (b) very weak or no labeling in the bacteroids of senescent nodules, (c and d) moderate labeling in the mitochondria and cytoplasm of infected cells from mature nodules and (e) moderate labeling in the nuclei of an infected cell from a mature nodule. (f) A negative control obtained as described in Materials & Methods shows absence of labeling in bacteroids and other cellular compartments. b, bacteroid; c, cytoplasm; cw, cell wall; m, mitochondrion; n, nucleus; nu, nucleolus; v, vacuole. Bars, 1 μm (a, b, e, f); 0.5 μm (c, d).

Fig. 4 (a) Manganese-superoxide dismutase (MnSOD) activity in mitochondria and (b) alternative oxidase (AOX) mRNA level in young (Y), mature (M) and senescent (S) bean nodules. In (a) values are means ± SE of three replicates, each from nodules of 15 plants. Means denoted by the same letter are not significantly different at $P<0.05$ based on Duncan's multiple range test. In (b) values are means ± SE of four replicates, each corresponding to RNA extractions from nodules of four different sets of plants. Values were routinely normalized with respect to *ubiquitin*, although expression patterns were confirmed with other reference genes, as outlined in Materials & Methods. *R* values >2 (upregulation) with respect to the control ($R=1$ for young nodules) were considered to be significant and marked with an asterisk.

Fig. 5 Gene expression levels of selected peroxiredoxins and thioredoxins in young (Y), mature (M) and senescent (S) bean nodules. Mitochondrial enzymes: PrxIIF and Trx*o*; cytosolic enzymes: PrxIIB, Trx*h1* and Trx*h4*. Values are means ± SE of four replicates, each corresponding to RNA extractions from nodules of four different sets of plants. Values were routinely normalized with respect to *ubiquitin*, although expression patterns were confirmed with other reference genes as outlined in Materials & Methods. *R* values >2 (upregulation) or <0.5 (downregulation) with respect to the control ($R=1$ for young nodules) were considered to be significant and marked with an asterisk.

Fig. 6 Percentage of methionine sulfoxide (MetSO) to total methionine residues [MetSO/(Met + MetSO) x 100] of the glutamine synthetase isoform GS-N1 in the cytosol. GS-N1 contains two methionine residues at positions 31 and 33 that are prone to sulfoxidation. The peptide containing Met-31 and Met-33 shows differential susceptibility in young (Y), mature (M) and senescent (S) bean nodules. For quantification, it was possible to distinguish between no-oxidation, single MetSO and doubly MetSO. Ratios of the abundance of single MetSO and doubly MetSO peptides with respect to the total abundance of the three peptide species were calculated. Values are means ± SE of five replicates and those denoted by the same letter are not significantly different at $P<0.05$ based on Duncan's multiple range test.

Table 1 Relative abundance of glutathione in infected cells of pea nodules

Developmental stage[1]	Mitochondria	Cytosol	Bacteroids	Nucleus
Young	6.2 ± 0.9 a	4.0 ± 0.6 a	81.8 ± 6.9 a	2.1 ± 0.3 a
Mature	2.9 ± 0.3 b	15.5 ± 1.2 b	129.1 ± 9.0 b	3.8 ± 0.3 b
Senescent	nd[2]	nd	6.4 ± 0.6 c	nd

[1] Data (gold particles per μm^2) are means ± SE (*n*= 40 for mitochondria and bacteroids; *n*= 30 for cytosol, *n*= 25 for nuclei) and those denoted by different letters within the same columns are significantly different at $P<0.05$ based on Duncan's multiple range test.
[2] nd, not detectable..

Table 2 Proteins of bean nodule mitochondria that are induced or repressed with aging

Protein	TC[1]	UniProt[2]	Young		Mature		Senescent	
Amino acid metabolism								
Glutamate dehydrogenase 1	TC34875	Q5F2M9	2.5	a	2.5	a	1.0	b
NADH glutamate synthase precursor	NP7938775	Q93WZ7	0.3	a	1.6	b	0.0	a
Serine hydroxymethyltransferase, mitochondrial	TC38452	P50433	2.5	a	2.2	ab	1.0	b
Homoserine kinase	TC37342	Q9XEE0	3.3	a	3.2	a	0.4	b
D-3-phosphoglycerate dehydrogenase	TC44520	O04130	4.9	a	5.0	a	3.7	b
Isovaleryl-CoA dehydrogenase precursor	GW903826	Q9SM62	2.5	a	2.7	a	1.2	b
Aspartate aminotransferase	TC32236	Q8HQQ0	2.3	a	2.3	a	0.4	b
Antioxidant / redox								
Ascorbate peroxidase, mitochondrial/chloroplastic	TC38704	Q5QHW7	3.1	a	2.0	a	0.7	b
Peroxidase 1	FD786965	Q9XFL3	0.4	ab	1.2	a	0.0	b
Catalase	TC42537	O48561	2.6	a	3.7	b	3.6	b
Stress								
Heat shock 70 kDa protein, mitochondrial precursor	TC32170	Q01899	4.8	a	4.5	a	3.6	b
Heat shock 10 kDa protein	TC39508	A3FPF3	3.6	a	3.5	a	2.1	b
Hypersensitive-induced response protein	TC32777	Q6UNT3	2.1	a	3.1	b	3.3	b
TCA / oxidative phosphorylation								
Pyruvate dehydrogenase E1 component subunit alpha	TC41304	Q4JIY3	2.8	a	3.1	a	1.0	b
Pyruvate dehydrogenase E1 beta subunit isoform 2	TC34095	Q9ZQY2	4.2	a	3.9	a	3.5	b
Malate dehydrogenase, nodule-enhanced	TC37821	O81278	3.2	a	2.7	a	1.0	b
2-Oxoglutarate dehydrogenase, mitochondrial-like	CV532177	Q9M2T8	2.5	a	2.8	a	0.5	b
2-Oxoglutarate dehydrogenase, mitochondrial	TC34429	Q3E9W2	3.0	a	3.1	a	1.3	b
Fumarate hydratase 1	TC32848	Q10LR5	3.1	a	3.0	a	1.1	b
Complex I (NADH dehydrogenase)	TC46103	Q43840	2.1	a	1.9	a	0.5	b
Complex I (NADH dehydrogenase)	TC37286	Q5Z7T4	3.8	a	3.2	b	2.4	c
Complex I (NADH dehydrogenase [ubiquinone])	TC32737	Q9SK66	4.0	a	3.3	a	1.5	b
Complex I (NADH-ubiquinone oxidoreductase)	TC37990	Q7ILE4	2.5	a	2.4	a	1.0	b
Complex III (ubiquinol-cytochrome *c* reductase Fe-S subunit)	TC44534	P49729	2.1	a	2.0	a	0.0	b
Cytochrome *c* oxidase subunit Vb	TC32892	Q0KKQ3	1.8	a	0.7	ab	0.0	b
ATPase mitochondrial F1-gamma subunit	TC34331	Q59I53	4.2	a	4.1	a	3.2	b
Nucleotide metabolism / ureide biosynthesis								
Aminoimidazole ribonucleotide carboxylase	TC43042	Q8W197	1.7	ab	2.7	a	1.1	b
Ribose-phosphate pyrophosphokinase 1	TC35588	Q42581	1.0	a	2.5	b	0.0	c
Ribose-phosphate pyrophosphokinase 2	TC35414	Q42583	1.0	a	2.3	b	0.0	c
Phosphoribosylformylglycinamidine cyclo-ligase, chloroplast/mitochondrial	TC35536	P52424	3.7	a	4.2	a	2.3	b
Phosphoribosylpyrophosphate amidotransferase	TC36958	O81358	0.6	a	1.5	b	0.2	a
Adenylosuccinate-AMP lyase	TC36068	Q8VZX0	1.3	a	1.4	a	0.2	b
Formylglycinamide ribonucleotide amidotransferase	TC45362	Q8VYU2	0.6	ab	1.3	a	0.0	b
Dihydropyrimidine dehydrogenase	TC33820	Q6Z744	3.2	a	3.7	a	2.2	b
Transport								
Voltage-gated anion channel, mitochondria	TC34262	Q6W2J2	3.0	a	2.6	a	0.8	b
Voltage-dependent anion channel	TC45536	Q6W2J3	3.4	a	3.1	a	2.3	b
Mitochondrial import receptor subunit TOM20, putative	TC36486	P92792	2.5	a	2.3	a	0.0	b
Nodulins								
Nodulin 41	TC36046	G1FTR5	4.6	a	4.5	a	2.8	b
Mitochondrial processing peptidase beta subunit	TC36407	Q9AXQ2	4.7	a	4.7	a	4.0	b
Protein degradation								
Subtilisin-like protease	TC37598	Q9ZUF6	2.8	a	0.9	b	0.7	b
Serine carboxypeptidase-like protein	TC36390	Q8L7B2	1.2	a	0.2	ab	0.0	b
Metal homeostasis								
Ferritin-2, chloroplast precursor	TC32629	Q41709	2.0	a	1.1	b	0.0	c
Other								
CBS domain-containing protein	TC36694	Q0IPT3	3.5	a	3.3	a	0.0	b
CXE carboxylesterase	TC37468	Q0ZPW9	1.4	a	2.8	b	3.1	b
Prohibitin-1, mitochondrial	TC35529	O04361	3.6	a	3.4	a	2.5	b
Glutamine cyclotransferase precursor	TC35679	O81226	2.5	a	2.4	a	1.0	b
Enoyl-ACP reductase precursor	TC41680	O04945	2.0	a	2.2	a	0.0	b
Glycine-rich RNA-binding protein PsGRBP	TC45102	P93486	2.2	a	1.2	b	0.3	c

Values ($\log_2$ of the number of spectral counts) are means of six biological replicates from two series of plants grown independently. Means denoted by the same letter are not significantly different at $P < 0.05$ according to Duncan's multiple range test.

[1] Tentative consensus (TC) sequences according to the DFCI Bean Gene Index (4.0).

[2] UniProt accessions (UniRef100).

Table 3 Proteins of bean nodule cytosol that are induced or repressed with aging

Protein	TC[1]	UniProt[2]	Young		Mature		Senescent	
Nitrogen fixation								
Leghemoglobin	TC36622	Q03972	7.4	a	6.5	a	3.9	b
Amino acid metabolism								
Glutamine synthetase PR-1	TC35865	P04770	1.9	ab	2.8	a	1.5	b
Cysteine synthase	TC36772	A3RM06	2.1	a	1.4	ab	0.2	b
Methionine synthase	TC42435	Q71EW8	2.1	a	0.9	ab	0.2	b
S-adenosylmethionine synthetase	TC35526	A4PU48	4.2	a	3.4	a	1.0	b
Carbohydrate metabolism								
Fructose-bisphosphate aldolase, cytosolic	TC36120	O65735	4.9	a	3.2	ab	1.0	b
Glyceraldehyde-3-dehydrogenase C subunit	TC37464	Q07CZ3	3.1	a	3.9	a	1.0	b
Glyceraldehyde-3-phosphate dehydrogenase, cytosolic	TC33650	P34921	1.6	a	2.1	a	0.0	b
Enolase	TC44689	Q6RIB7	4.1	a	4.5	a	2.0	b
Triosephosphate isomerase	TC33325	Q5JZZ3	2.2	a	1.8	a	0.0	b
Fructokinase-like protein	TC43195	Q9LNE3	3.4	a	3.1	a	1.0	b
Sucrose synthase	TC35849	Q8GTA3	4.9	a	4.7	a	3.0	b
UDP-glucose pyrophosphorylase	TC36416	Q8W557	0.9	a	0.6	ab	0.0	b
Carbon fixation								
Phospho*enol*pyruvate carboxylase	TC34225	Q9ZS53	2.8	a	1.4	b	0.0	c
Carbonic anhydrase	TC36859	Q9AU12	1.9	a	1.1	a	0.0	b
Antioxidant/Redox								
Ascorbate peroxidase, cytosolic	TC32379	Q9XG11	3.8	a	3.2	a	1.1	b
Superoxide dismutase [Cu-Zn]	FE899597	Q41712	2.4	a	1.1	b	0.2	b
Peroxiredoxin	TC37614	F2WVP3	0.9	a	0.6	ab	0.0	b
Heme oxygenase 1	TC44951	Q06H32	0.6	a	2.0	b	1.7	b
Monodehydroascorbate reductase	TC33312	Q94FX1	1.9	a	2.7	a	0.4	b
Protein synthesis								
Ribosomal protein 60S acidic P2	TC38965	Q66PF9	2.2	a	0	b	0.0	b
Ribosomal protein S8	TC41325	A8QJ72	1.7	a	0.9	ab	0.0	b
Ribosomal protein 40S SA	TC41632	Q3HRZ6	1.1	a	0	b	0.0	b
Ribosomal protein 40S S15-like protein	TC35497	O22518	1.2	a	0.6	ab	0.0	b
Eukaryotic initiation factor 4A-10-like	TC43412	Q9FY64	0.7	ab	1.4	a	0.0	b
Translation protein SH3-like	CV531340	A9PD17	1.2	a	0.5	ab	0.0	b
Putative translation elongation factor	TC44261	Q2HRD6	3.1	a	2.6	a	0.7	b
Predicted elongation factor 1-beta-1 like	TC34901	Q9ASR1	3.0	a	1.0	b	0.0	b
Stress								
Pathogenesis-related protein 1	FG229903	Q9SCX3	3.0	a	1.3	ab	0.7	b
Heat shock 70 kDa cognate protein 1	TC45292	P25985	2.8	a	2.0	ab	0.3	b
Heat shock 70 kDa cognate protein 2	TC35538	Q5QHT4	2.7	a	1.8	a	0.0	b
Heat shock 70 kDa cognate protein 3	TC39659	Q5QHT3	2.5	a	2.1	a	0.0	b
Molecular chaperone Hsp90-1	TC33556	Q5QHT2	3.3	a	2.9	a	1.2	b
Peptidyl-prolyl *cis-trans* isomerase	GW885607	Q6UJX4	2.8	a	1.3	b	0.7	b
TCA								
Malate dehydrogenase	TC32699	Q41119	3.4	a	3.1	a	1.5	b
Nucleotide metabolism								
Adenylate kinase B	TC32308	Q2PYY8	2.2	a	2.4	a	1.0	b
Ribonucleoside hydrolase	TC35502	Q08480	1.6	ab	1.9	a	0.7	b
Signaling								
14-3-3 protein	TC35424	Q6ZJ05	2.5	a	3.0	a	0.7	b
14-3-3-like protein A	TC33838	Q93XW1	1.9	ab	2.7	a	0.7	b
14-3-3-like protein C	TC34878	Q96450	1.0	ab	1.5	a	0.0	b
Transport								
ATPase	TC42561	Q96452	2.5	a	1.4	a	0.0	b
Cell wall/ Cell organization								
Actin	TC33350	O81221	3.2	a	1.5	b	0.0	c
Actin-11	TC35707	P53496	3.1	a	1.8	b	0.2	c
Tubulin alpha-3 chain	TC33053	Q9ZRR5	2.6	a	0.9	b	0.0	b
Tubulin beta-1 chain	TC43169	P37392	3.5	a	2.3	b	0.3	c
Tubulin beta-1 chain	TC42085	A7KQH3	3.7	a	2.3	b	0.3	c
Tubulin beta-3 chain	TC35683	Q40665	3.4	a	1.9	b	0.3	c
Tubulin A	TC32424	Q2TFP2	1.2	a	1.7	a	0.2	b
Nodulins								
Nodulin 6l	TC38826	Q8S4Q4	1.4	a	2.0	a	0.0	b
Nodulin 30 precursor	TC38855	Q41121	2.9	a	1.2	b	0.0	c
Nodulin 41	TC36046	G1FTR5	4.3	a	3.7	a	1.1	b
Hormone metabolism								
Lipoxygenase	TC32566	Q9FQF9	2.3	a	2.6	a	0.7	b
Other								
CXE carboxylesterase	TC37468	Q0ZPW9	0.0	a	1.2	b	0.5	ab
Inorganic pyrophosphatase	TC34001	Q949J1	1.6	a	0.8	ab	0.2	b

Values (log_2 of the number of spectral counts) are means of five biological replicates, each from a different series of plants grown independently. Means denoted by the same letter are not significantly different at $P < 0.05$ according to Duncan's multiple range test.

[1] Tentative consensus (TC) sequences according to the DFCI Bean Gene Index (4.0).

[2] UniProt accessions (UniRef100).

Table S1 Primers used for qRT-PCR analyses

Gene	Forward	Reverse
Actin	AGC TGT GCT TTC CCT TTA CG	TTC ATA GAT GGG GAC CGT GT
*PP2A**	GAG AAC AAC GAC GAT GAC GA	CTC CGA CGT AGG GAA TGA AA
Ubiquitin	GCT TCG TGG TGG AAT GCA GAT	TTG TAG TCT GCC AAG GTG CGA
*UBQCE**	CCC AGC TTG GAC ACT TCA AT	AGC CTC TAA CAT CGC CTG AA
PrxIIF	GCT TCA AGC CAA AGA GGC TA	AAT GCA CCC GAG AGA TCA GT
PrxIIB	TTG CCA ATG TTG AAA GTG GA	GGG GAC ATC AAA GAA CCA AC
Trxh1	GGT GGT GCA GAA AGT TCC AT	TCC AAG CTG AAA TCA TCC AA
Trxh4	GGA CGA GCT CGA GAA GAA GA	TTT GTT TTC CTT CCT TGA AAA G
Trxo	TGG GCA AAT TGC AGA TTA CA	GGT CAA TCG TGC AAC ATC AG
AOX-1a	TGG TGG GTT ACC TTG AGG AG	GGA GCT GGC ACA TTT TGA AT

**PP2A, protein phosphatase 2A*; *UBQCE, ubiquitin conjugating enzyme.*

Fig. 1

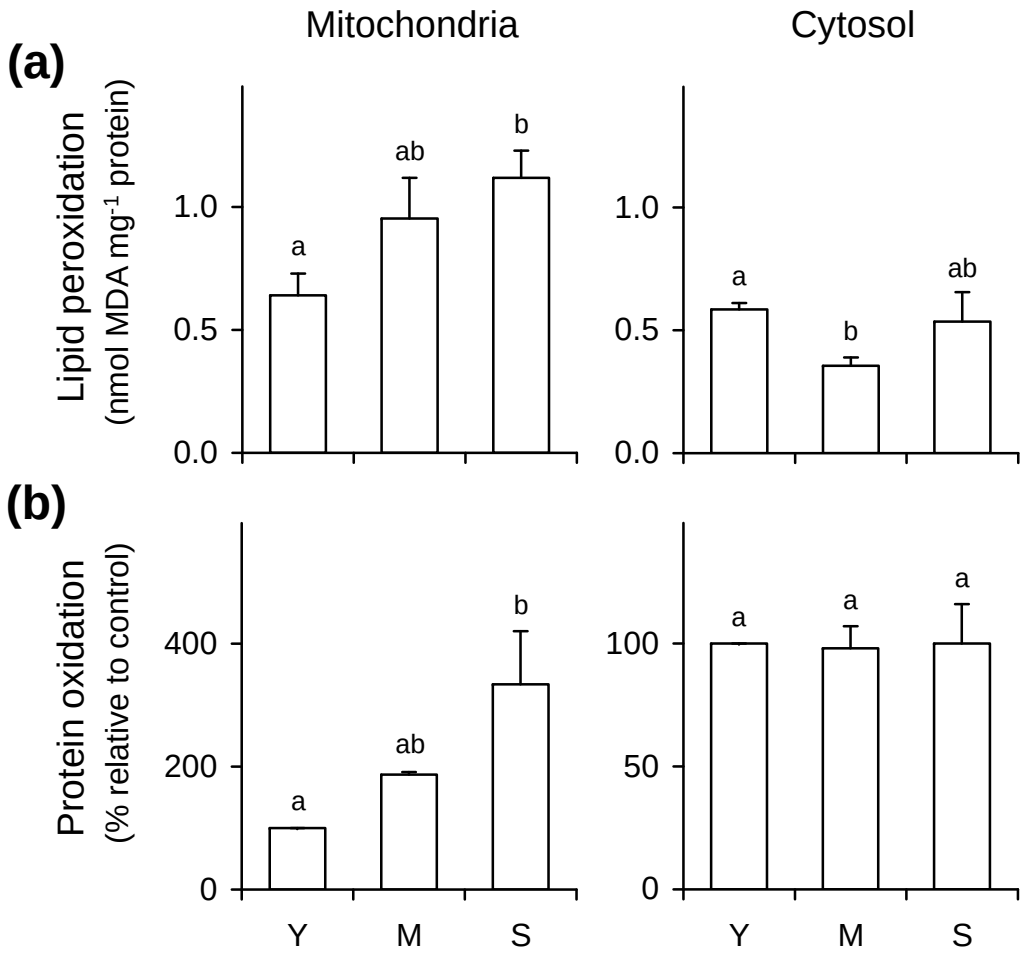
Mitochondria
Cytosol
(a)
Lipid peroxidation
(nmol MDA mg-1 protein)
1.0
0.5
0.0
a
ab
b
a
b
ab
(b)
Protein oxidation
(% relative to control)
400
200
0
100
50
a
ab
b
a
a
a
Y
M
S

Fig. 2

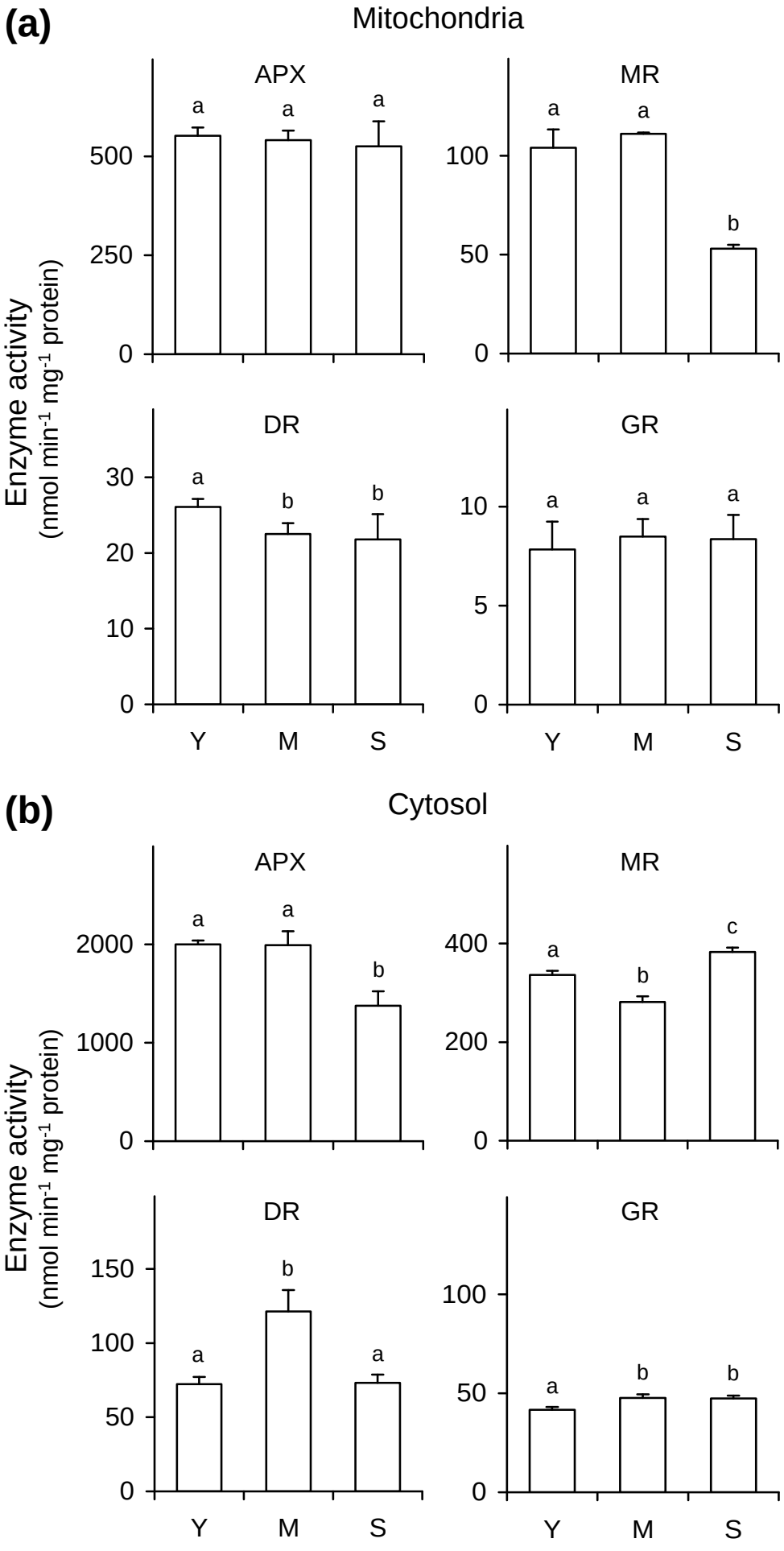
(a)
Mitochondria
APX
MR
DR
GR
Enzyme activity
(nmol min-1 mg-1 protein)
Y
M
S
(b)
Cytosol
APX
MR
DR
GR
Enzyme activity
(nmol min-1 mg-1 protein)
Y
M
S

Fig. 3

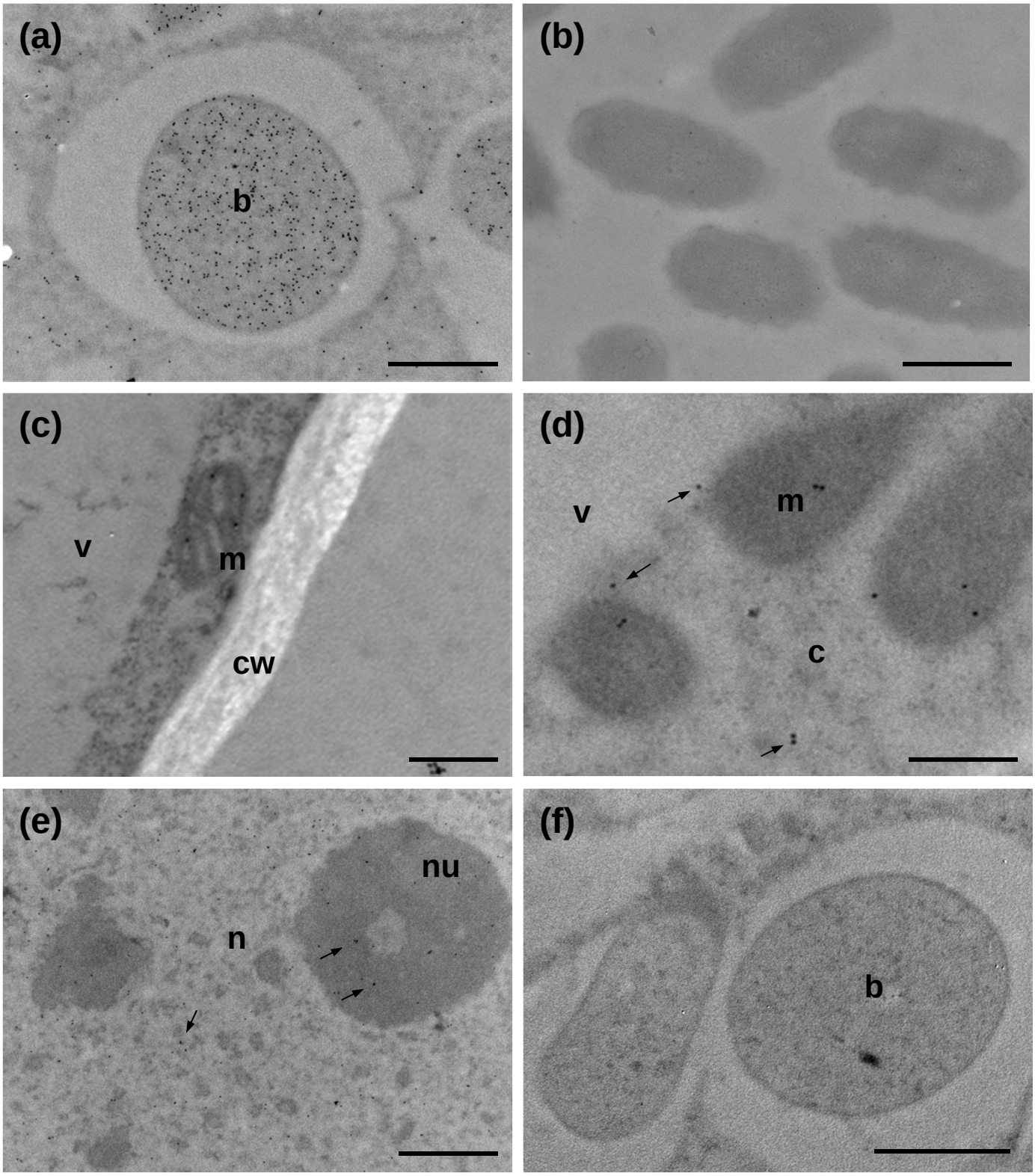

Fig. 4

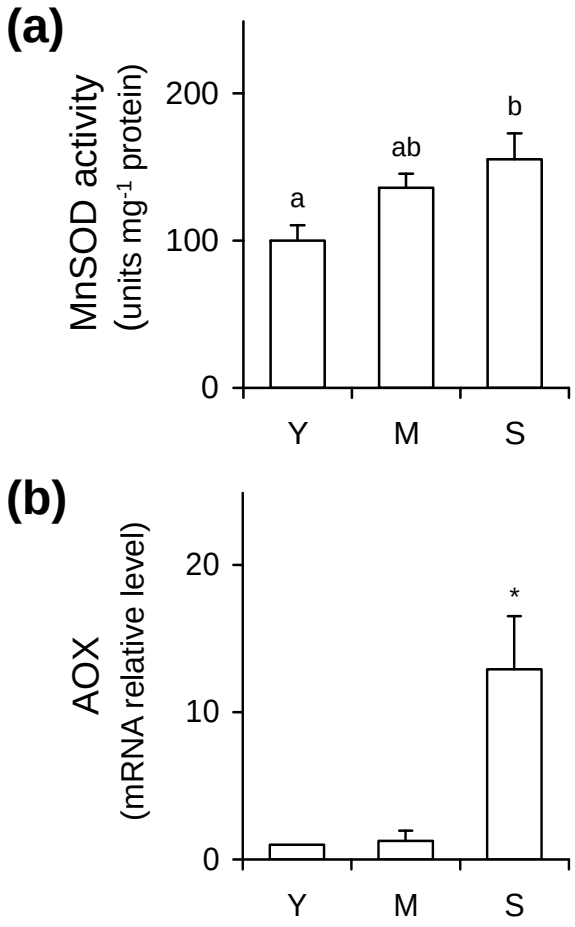
(a)
MnSOD activity
(units mg-1 protein)
200
100
0
a
ab
b
Y
M
S
(b)
AOX
(mRNA relative level)
20
10
0
*
Y
M
S

Fig. 5

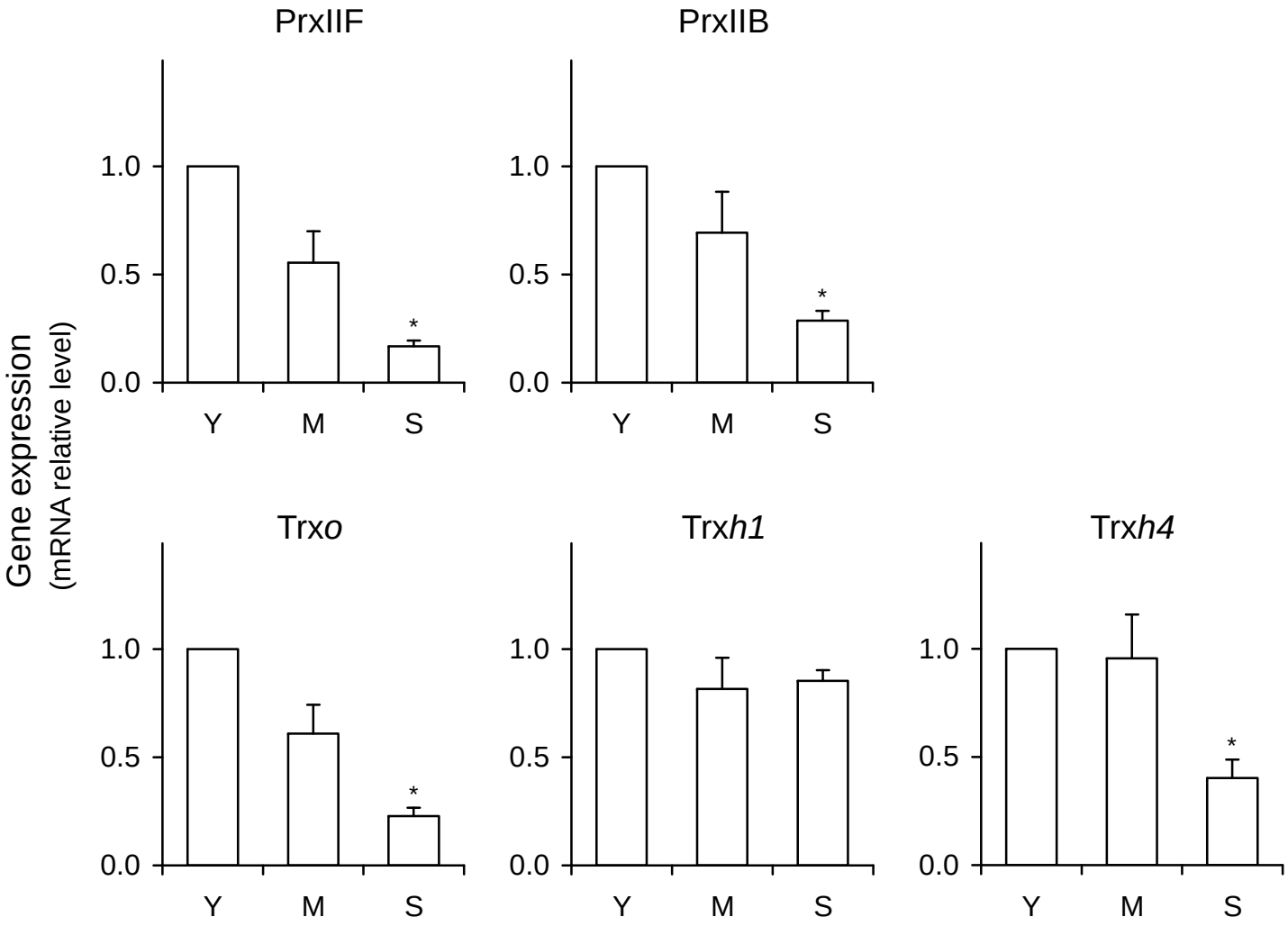
PrxIIF
PrxIIB
Trxo
Trxh1
Trxh4
Gene expression
(mRNA relative level)
1.0
0.5
0.0
Y
M
S
*

Fig. 6

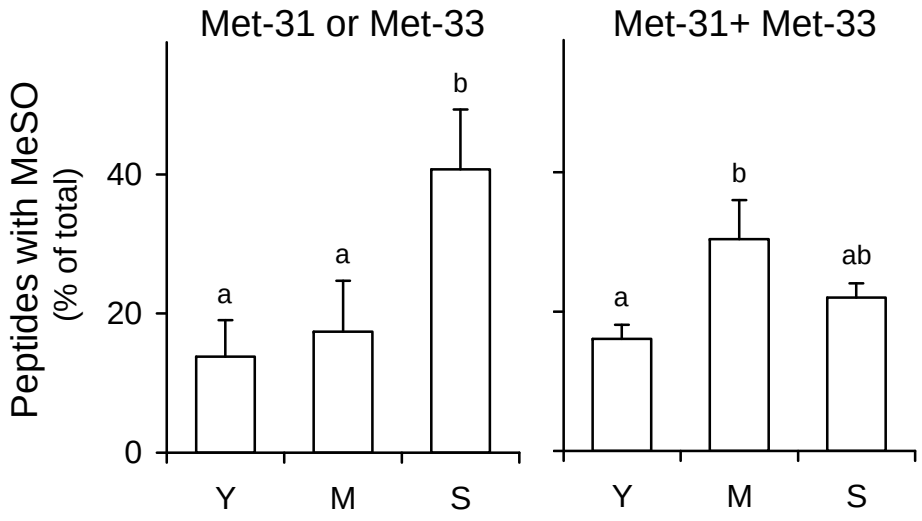
Met-31 or Met-33
Met-31+ Met-33
Peptides with MeSO
(% of total)
0
20
40
a
a
b
a
b
ab
Y
M
S
Y
M
S

Fig. S1

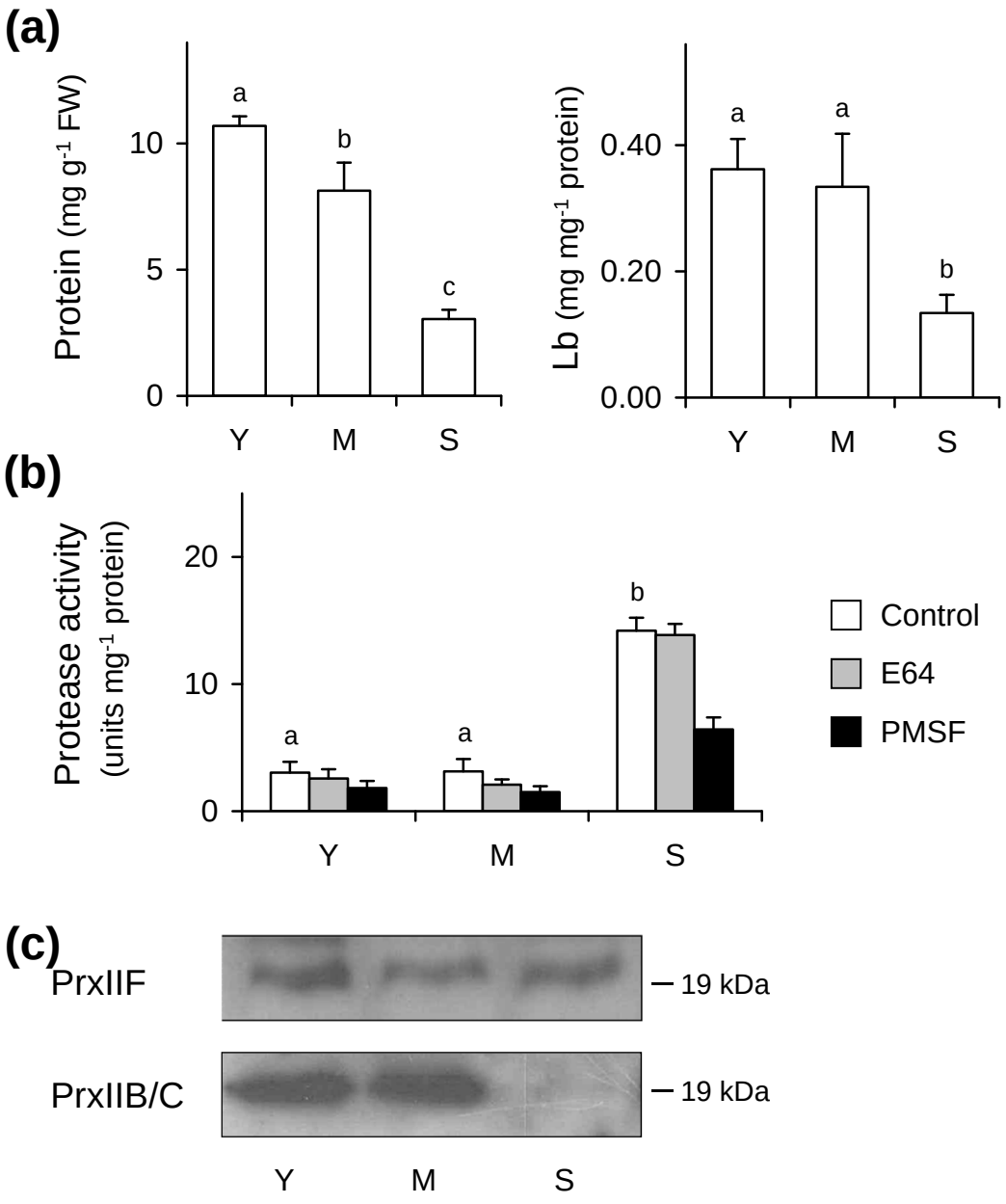
(a)
Protein (mg g-1 FW)
10
5
0
a
b
c
Y
M
S
Lb (mg mg-1 protein)
0.40
0.20
0.00
a
a
b
Y
M
S
(b)
Protease activity
(units mg-1 protein)
20
10
0
a
a
b
Y
M
S
Control
E64
PMSF
(c)
PrxIIF
19 kDa
PrxIIB/C
19 kDa
Y
M
S

Fig. S2